ISSN 1674-1056
http://cpb.iphy.ac.cn
http://iopscience.iop.org/cpb
中国物理 B
Chinese Physics
中国物理 Chinese Physics B

Double-slit interference of a relativistic vortex laser

Hao Zhang(张浩), Bai-Fei Shen(沈百飞), Lin-Gang Zhang(张林港)

Citation: Chin. Phys. B . 2019, 28(1): 014702. **doi:** 10.1088/1674-1056/28/1/014702
Journal homepage: http://cpb.iphy.ac.cn; http://iopscience.iop.org/cpb

What follows is a list of articles you may be interested in

Observation of double pseudowaves in an ion-beam-plasma system

Zi-An Wei(卫子安), Jin-Xiu Ma(马锦秀), Kai-Yang Yi(弋开阳)

Chin. Phys. B . 2018, 27(8): 085201. **doi:** 10.1088/1674-1056/27/8/085201

Upstream ion wave excitation in an ion-beam-plasma system

Kai-Yang Yi(弋开阳), Jin-Xiu Ma(马锦秀), Zi-An Wei(卫子安), Zheng-Yuan Li(李政元)

Chin. Phys. B . 2018, 27(5): 055201. **doi:** 10.1088/1674-1056/27/5/055201

Production of intense attosecond vector beam pulse trains based on harmonics

Han Yu-Jing, Liao Guo-Qian, Chen Li-Ming, Li Yu-Tong, Wang Wei-Min, Zhang Jie

Chin. Phys. B . 2015, 24(11): 115203. **doi:** 10.1088/1674-1056/24/11/115203

Plural interactions of space charge wave harmonics during the development of two-stream instability

Victor Kulish, Alexander Lysenko, Michael Rombovsky, Vitaliy Koval, Iurii Volk

Chin. Phys. B . 2015, 24(9): 095201. **doi:** 10.1088/1674-1056/24/9/095201

High-order optical vortex harmonics generated by relativistic femtosecond laser pulse

Han Yu-Jing, Liao Guo-Qian, Chen Li-Ming, Li Yu-Tong, Wang Wei-Min, Zhang Jie

Chin. Phys. B . 2015, 24(6): 065202. **doi:** 10.1088/1674-1056/24/6/065202

Double-slit interference of a relativistic vortex laser*

Hao Zhang(张浩)[1,2], Bai-Fei Shen(沈百飞)[1,2,3,†], and Lin-Gang Zhang(张林港)[1,‡]

[1] State Key Laboratory of High Field Laser Physics, Shanghai Institute of Optics and Fine Mechanics, Chinese Academy of Sciences, Shanghai 201800, China

[2] University of Chinese Academy of Sciences, Beijing 100049, China

[3] Department of Physics, Shanghai Normal University, Shanghai 200234, China

(Received 10 September 2018; revised manuscript received 24 October 2018; published online 30 December 2018)

The interference of a relativistic vortex laser is investigated for the case when a linearly polarized Laguerre–Gaussian pulse impinges on a double-slit solid target. Three-dimensional particle-in-cell simulation results show that the interference fringes of high-order harmonics are twisted, similar to that of the fundamental vortex laser. The twisting order of the interference pattern is determined by the order of the vortex high-order harmonics, which can be explained by the classic double-slit interference models. The usual double-slit interference has been extended to the regime of relativistic intensity, which may have potential applications for measuring the topological charge of vortex high-order harmonics.

Keywords: optical vortices, fringes analysis, harmonics

PACS: 47.32.cb, 52.35.–g, 42.25.Hz **DOI:** 10.1088/1674-1056/28/1/014702

1. Introduction

Vortex beams are light beams with helical wavefronts.[1,2] The characteristic helical phase profiles of vortex beams are described by the phase term $\exp(il\theta)$, where θ is the azimuthal angle and l is the topological charge (TC). The total phase accumulated in one full annular loop is $2l\pi$, and the average orbital angular momentum (OAM) carried by a l-order linearly polarized optical vortex beam is $l\hbar$ per photon, where $\hbar$ is the reduced Planck's constant. Owing to their unique characteristics, vortex beams have been used in many fields, such as information encoding,[3] optical manipulation,[4,5] stimulated emission depletion microscopy,[6] and optical metrology.[7,8]

Interference is a key aspect demonstrating the wave characteristic. Double-slit is one of the most popular interference experiments to show the wave nature of light,[9] electrons,[10,11] neutrons,[12] and atoms.[13] Generally, the double-slit interference pattern from a Gaussian beam is bright and dark straight lines. Curiously, when the laser is a vortex beam, the double-slit interference fringes are twisted in the central region, that is, the fringes at the bottom zone of the interference pattern shift relative to the ones at the upper zone.[14–16] The twisting order, which refers to the shift number of the fringes, is decided by the TC of the vortex beam. Furthermore, the shift direction of the twisting fringes depends on the sign of the TC. Then the TC can be evaluated from the twisted interference pattern of the vortex beam through a double-slit target. However, current studies have mainly investigated diffraction or interference of vortex beams under the non-relativistic mechanism.[14–16] For relativistic vortex beams, nonlinear effects will appear in laser–plasma interaction.[17,18] Recently, the optical vortex has been applied in strong field physics, high-energy photon generation with large OAM by high harmonic generation.[17,18] Simulation results by Zhang *et al.* showed that intense vortex high-order harmonics can be generated when a linearly polarized fundamental vortex pulse impinges on a plane solid plasma target.[17] The field of intense vortex high-order harmonics has an intertwined helical structure and the number of intertwined helices equals the TC of intense vortex high-order harmonics, which also equals the order of intense vortex high-order harmonics. The vortex oscillating mirror (VOM) model proposed by Zhang *et al.* demonstrated that the OAM of intense vortex high-order harmonics is conserved in the interaction of lasers and plane solid plasma targets. Subsequent experimental results performed by Denoeud *et al.* verified this conservation rule.[19] The targets in previous studies were plane solid targets or double-slit targets under the non-relativistic mechanism.[14–19] If the solid target is a double-slit target under relativistic mechanism, such a situation has not been studied in much detail.

In this study, we investigate the interference properties of relativistic vortex lasers by impinging a lower-order vortex pulse to a well-designed double-slit plasma solid target. Intense vortex high-order harmonics can be generated and then

*Project supported by the National Natural Science Foundation of China (Grant Nos. 11335013, 11575274, 11674339, and 61805266), the Strategic Priority Research Program of the Chinese Academy of Sciences (Grant No. XDB16), the Ministry of Science and Technology of the People's Republic of China (Grant Nos. 2016YFA0401102 and 2018YFA0404803), and the Innovation Program of the Shanghai Municipal Education Commission, China (Grant No. 201701070002E00032).

†Corresponding author. E-mail: bfshen@mail.shcnc.ac.cn

‡Corresponding author. E-mail: lgzhang@siom.ac.cn

© 2019 Chinese Physical Society and IOP Publishing Ltd

interfere in the transmitted light direction. We find that the interference fringes for both the fundamental and the third-order vortex laser are twisted in the viewer screen. The twisting order of interference fringes for both fundamental and the third-order vortex lasers are decided by the order of the harmonics. The classical double-slit interference models are employed to explain the simulation results. We extend the usual double-slit interference to the regime of relativistic intensities and help to check the conservation of OAM when a relativistic vortex laser interacts with a double-slit solid target, that is, the TC of intense qth vortex high-order harmonics would be equal to q times of the TC of the fundamental vortex laser. The double-slit interference of vortex high-order harmonics may have potential applications for measuring their TC.

2. PIC simulation

The proposed scheme was studied with three-dimensional (3D) particle-in-cell (PIC) simulations based on EPOCH code.[20] The setup is shown in Fig. 1. A driving p-polarized Laguerre–Gaussian (LG) laser irradiates a double-slit solid plasma target. The field amplitude of an LG laser with mode (l, p) is given by

$$E\left(\mathrm{LG}_p^l\right) = a(-1)^p \exp\left[-\frac{r^2}{r_0^2}\right]\left(\frac{r\sqrt{2}}{r_0}\right)^{|l|} \times \mathrm{L}_p^l\left(\frac{2r^2}{r_0^2}\right)\exp(\mathrm{i}l\theta)\sin^2\left(\frac{\pi t}{2t_0}\right), \quad (1)$$

where $a = eA/m_\mathrm{e}c^2$ is the normalized laser vector potential, A is the vector potential, c is the speed of light in vacuum, ω is the frequency of the input beam, m_e is the electron mass, e is the electron charge, $r = \sqrt{y^2+z^2}$ is the radius, L_p^l is the generalized Laguerre polynomial, and p is the number of radial nodes in the intensity distribution.[1,2] In our simulation, we used the LG_0^1 mode, with $\mathrm{L}_0^1 = 1$, $r = 5\lambda$, and $t = 6T$, where T is the driving laser period and $\lambda = 0.8$ μm is the wavelength of the driving laser. The intense LG laser has an amplitude $a = 5$, corresponding to a peak laser intensity of 5.4×10^{19} W/cm^2. The size of the simulation box was $20\lambda\times15\lambda\times15\lambda$, corresponding to a window of $600\times450\times450$ cells in the $x\times y\times z$ directions, where each cell has one electron and proton. At $t = 0$, the laser pulse enters the simulation box from the left boundary. The double-slit target located at $5\lambda < x < 6\lambda$ and $-7.5\lambda < y(z) < 7.5\lambda$ initially has a uniform cold electron density of $10n_\mathrm{c}$. Each slit has a width of $b = 0.5\lambda$ with a spacing between slit edges of $d = 2.5\lambda$. The distance between the double-slit target and the viewer screen is $D = 10\lambda$.

The distributions of E_y in the x–y plane of $z = 0$ are shown in Fig. 2(a) at $t = 56$ fs when the vortex laser passes through the double-slit target. Figure 2(b) shows the transverse intensity profiles of the fundamental laser in the y–z plane integrated over $x = 16$–20λ, where $x = 16\lambda$ is the location of the viewer screen. The interference pattern in Fig. 2(b) is quite different from the usual interference pattern of a double slit for a Gaussian laser. Generally, for a Gaussian laser, the interference fringes are straight lines with equal line space. Also, as each slit has a width b, the pattern has a principal maximum intensity and a series of peaks of decreasing intensity. However, for a vortex laser, the interference fringes are not straight lines. As seen in Fig. 2(b), for one single fringe, the upper zone of the fringe shifts to one position along z axis while the bottom zone shifts to the opposite, and thus the fringe twists in the central region. For a better understanding of this shift, we select two points A and A' symmetrical to the y axis ($y = \pm3.99\lambda$) in one single fringe. The z coordinates of the points are selected to the maximum intensity point of the fringe at $y = \pm3.99\lambda$, respectively. Two yellow dashed lines are drawn cross A and A', from which one can see that the interference bright fringe of the vortex laser at the upper zone of the interference pattern does not align with the corresponding bright one at the bottom zone. The bright fringe at the bottom zone of the interference pattern has been shifted about one interference order from left to right compared with the bright one corresponding to the upper zone of the interference pattern.

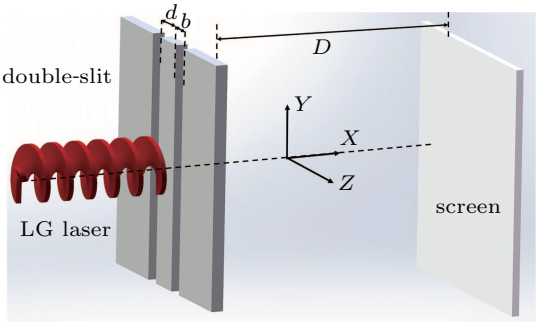


Fig. 1. An intense LG pulse irradiating a double-slit target, where each slit has a width $b = 0.5\lambda$ and a spacing between slit edges of $d = 2.5\lambda$. The distance between the double-slit target and the viewer screen is $D = 10\lambda$.

The twisting order of the interference fringes of vortex beams is related to its TC. Because the laser in Fig. 2(b) is in fundamental LG_0^1 mode, corresponding to $l = 1$, the twisting order of the interference fringes in Fig. 2(b) is about 1. This simulation result of the fundamental LG laser agrees closely with those of previous studies in the regime of non-relativistic vortex lasers.[14–16]

However, in the regime of relativistic vortex lasers, intense high-order vortex harmonics will be generated, which is quite different from the usual double-slit interference in the non-relativistic regime.[17–19] Figure 2(c) shows the transverse intensity profiles of the interference pattern of the third vortex harmonics in the y–z plane integrated over $x = 16$–20λ. According to the simulation results, the peak intensity for the third vortex harmonics is about 1.6×10^{17} W/cm^2, which is close to the relativistic regime. The interference of the fifth

or higher order vortex harmonics have been considered by parameters scan, but their interference patterns are not obvious, and further theoretical analyses are required to explore the interference physics of higher-order vortex harmonics. The energy of each photon for the third vortex harmonics is $3\hbar\omega$ on the basis of the energy conversation law. One may wonder whether the OAM of the third vortex harmonics is also conserved in the non-linear laser interaction with double-slit plasma. Fortunately, we can estimate the TC of the third-order vortex harmonics from the double-slit interference pattern.

Using the same method mentioned in Fig. 2(b), two points B and B' are also selected denoting the maximum intensity point for $y = 3.99\lambda$ and the maximum intensity point for $y = -3.99\lambda$ in one single fringe. The bright fringes in Fig. 2(c) at the bottom zone of the interference pattern have been shifted about three interference orders from left to right compared with the bright ones corresponding to the upper zone of the interference pattern. Therefore, the TC of the third vortex harmonics can be predicted to be about 3 from the twisting order of the pattern, which verifies the conservation rule for OAM in the laser's interaction with the double-slit plasma.

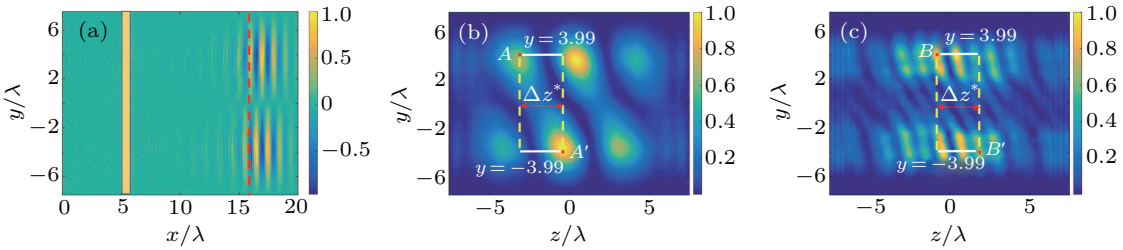


Fig. 2. (a) Normalized electric field E_y of the transmitted pulse in the x–y plane of $z = 0$ at $t = 56$ fs when the laser is transmitted. (b) Normalized transverse intensity distribution of the fundamental vortex laser in the y–z plane integrated over $x = 16$–20λ, where $x = 16\lambda$ is the location of the viewer screen. (c) Normalized transverse intensity distribution of the third vortex harmonics in the y–z plane integrated over $x = 16$–20λ.

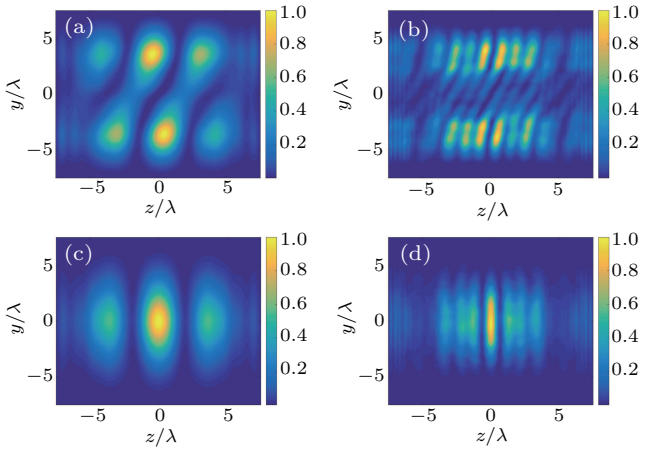


Fig. 3. Normalized transverse intensity distribution for different lasers in the y–z plane integrated over $x = 16$–20λ at $t = 56$ fs when the laser is transmitted. (a) Fundamental vortex laser with TC of negative sign. (b) Third vortex harmonics with TC of negative sign. (c) Fundamental Gaussian laser. (d) Third Gaussian harmonics.

As expected, when the sign of TC for a driving vortex laser is changed, the orientation of the twisting fringes is horizontally flipped, as shown in Figs. 3(a) and 3(b). Thus the TC of the fundamental and the third vortex harmonics can be estimated for $l = -1$ and $l = -3$ from the reversed twisting order. For comparison, when the driving laser becomes Gaussian mode, the interference fringes for both the fundamental (see Fig. 3(c)) and third harmonics (see Fig. 3(d)) are straight lines, which is simply the usual interference pattern of the double slit using a Gaussian laser. So far, the 3D PIC simulation results show that the interference pattern of a double-slit can be used to determine the TC and its sign of intense vortex high-order harmonics. We can deduce that the TC of qth intense vortex high-order harmonics equals q times of the TC of the fundamental intense vortex laser, thus verifying the conservation rule for OAM in laser interaction with double-slit plasma.

3. Theory

As the plasma target changes from plane surface to double slit, previous oscillating mirror (OM) or VOM models based on a plane target may not be applied to this case.[18,21,22] In our case, the generation mechanism of intense vortex high-order harmonics by double-slit is not clear. The intense vortex high-order harmonics may occur in the double-slit regime and then interfere after passing by the double-slit, which requires a future systematic study. Therefore, in this article we just focus mainly on the interference properties of intense vortex high-order harmonics and on whether the OAM of intense vortex high-order harmonics is conserved in laser interaction with double-slit plasma. The interference behavior of an intense vortex laser passing a double-slit can be explained by classical wave theory. Generally, the diffraction pattern for a Gaussian laser has a far-field intensity distribution given by[23]

$$I(z) = I_0 \mathrm{sinc}^2\left(\frac{\pi b z}{\lambda D}\right)\cos^2\left(\frac{\pi z(b+d)}{\lambda D}\right), \tag{2}$$

where λ is the wavelength of the incident light, $b+d$ is the separation of the two slits, and D is the distance from the slits to the viewer screen. This is often known as the far-field and is defined as being located at a distance greater than W^2/λ, where λ is the wavelength and W is the largest dimension in

the aperture.[24] In our case, we chose a distance $D = 10\lambda$ and a slit width $W = b + d = 3\lambda$. The distance $D = 10\lambda$ is greater than the value of $W^2/\lambda = 9\lambda$, which can be approximately regarded as far-field. Because the interference pattern is decided by both the single-slit width b (the sinc term in Eq. (2)) and the two-slit separation $b + d$ (the cos term in Eq. (2)), the pattern has a principal maximum intensity and a series of peaks of decreasing intensity, which can be seen in Figs. 3(c) and 3(d). The interference intensity $I(z)$ now is a function only of variable z, so the interference pattern for Gaussian laser is bright and dark straight lines.

When a vortex laser irradiates a double-slit, interference patterns become quite different.[14,16] An additional phase $\Delta\phi = l\pi + 2l \times \arctan[2y/(b+d)]$ should be added to the interference intensity distribution for the vortex laser, so that

$$\begin{aligned} I(y,z) &= I_0 \mathrm{sinc}^2\left(\frac{\pi bz}{\lambda D}\right)\cos^2\left(\frac{\pi z(b+d)}{\lambda D}+\frac{\Delta\phi}{2}\right) \\ &= I_0 \mathrm{sinc}^2\left(\frac{\pi bz}{\lambda D}\right)\cos^2\left(\frac{\pi z(b+d)}{\lambda D}\right. \\ &\quad \left.+\frac{l\pi}{2}+l\arctan\left(\frac{2y}{b+d}\right)\right). \end{aligned} \tag{3}$$

From Eq. (3), the interference intensity $I(y,z)$ is not only a function of variable z but also of y along the vertical direction, so the interference pattern for vortex laser is twisting fringes. The fringe space $\lambda D/(b+d)$ can be derived from Eq. (2) or Eq. (3). The twisting trace apart from the central region of the fringe can be described as[16]

$$z = \frac{l\lambda D}{(b+d)\pi}\arctan\left(\frac{2y}{b+d}\right). \tag{4}$$

For a given height of y^*, the TC value l can be described as

$$l = \frac{\Delta z^*(b+d)\pi}{2\lambda D\arctan\left(\frac{2y^*}{b+d}\right)}, \tag{5}$$

where Δz^* is the trace space of one single fringe at the given $\pm y^*$. In our case, for the fundamental and the third vortex harmonics in Fig. 2(b) and Fig. 2(c), six groups of points are selected to calculate their TC value based on Eq. (5). The TC results can be seen in Table 1.

Table 1. TC value of the fundamental and the third vortex harmonics.

	Points	y^*	Δz^*	TC	Average TC
Fundamental laser	(–3.06λ, 3.49λ) (–0.42λ, –3.49λ)	±3.49λ	2.64λ	1.07	1.07
	(–3.09λ, 3.99λ) (–0.36λ, –3.99λ)	±3.99λ	2.73λ	1.06	
	(–3.16λ, 4.49λ) (–0.32λ, –4.49λ)	±4.49λ	2.84λ	1.07	
Third harmonics	(–0.68λ, 3.49λ) (1.82λ, –3.49λ)	±3.49λ	2.50λ	3.03	3.10
	(–0.79λ, 3.99λ) (1.88λ, –3.99λ)	±3.99λ	2.67λ	3.12	
	(–0.85λ, 4.49λ) (1.92λ, –4.49λ)	±4.49λ	2.77λ	3.14	

From Table 1, we can see that the average values of TC for the fundamental and the third vortex are $\bar{l}_{1\omega} = 1.07$ and $\bar{l}_{3\omega} = 3.10$, which is rounded up to the integers 1 and 3, respectively. If the sign of the TC is changed, the orientation of the twisting fringes is reversed as expected according to Eq. (4). It has been verified that the interference features when a relativistic vortex laser passes through a double-slit target can be explained by this simple physical model, and the OAM of vortex high-order harmonics is conserved in laser interaction with double-slit plasma.

4. Conclusion

We expand the usual double-slit interference to the regime of relativistic intensities and help to check the conservation of OAM when a relativistic vortex laser interacts with a double-slit solid target. Vortex high-order harmonics are generated and then interfere in the regime of relativistic intensities, which is different from the case in the regime of non-relativistic intensities. The interference fringes for both fundamental vortex beam and high-order harmonics are twisted compared with usual straight interference fringes using a Gaussian laser. The classical double-slit interference models are employed to explain the PIC simulation results. It is shown that the TC of qth intense vortex high-order harmonics equals q times of the TC of the fundamental intense vortex laser, which may have potential applications for measuring the topological charge of vortex high-order harmonics.

References

[1] Allen L, Beijersbergen M W, Spreeuw R J C and Woerdman J P 1992 *Phys. Rev. A* **45** 8185
[2] Yuan X, Yu S and Urbach H P 2016 *Photonics Res.* **4** OVB1
[3] Wu J, Li H and Li Y 2007 *Opt. Eng.* **46** 019701
[4] Curtis J E, Koss B A and Grier D G 2002 *Opt. Commun.* **207** 169

[5] Otsu T, Ando T, Takiguchi Y, Ohtake Y, Toyata H and Itoh H 2015 *Sci. Rep.* **4** 4579
[6] Auksorius E, Boruah B R, Dunsby C, Lanigan P M P, Kennedy G, Neil M A A and French P M W 2008 *Opt. Lett.* **33** 113
[7] Wang W, Qiao Y, Ishijima R, Yokozeki T, Honda D, Matsuda A, Hanson S G and Takeda M 2008 *Opt. Express* **16** 13908
[8] Sato S, Fujimoto I, Kurihara T and Ando S 2008 *Proc. SPIE* **6877** 68770I
[9] Young T 1802 *Philos. Trans. R. Soc. London* **92** 387
[10] Jonsson C 1961 *Z. Phys.* **161** 454
[11] Jonsson C 1974 *Am. J. Phys.* **42** 4
[12] Zeilinger A, Gähler R, Shull C G, Treimer W and Mampe W 1988 *Rev. Mod. Phys.* **60** 1067
[13] Carnal O and Mlynek J 1991 *Phys. Rev. Lett.* **66** 2689
[14] Sztul H I and Alfano R R 2006 *Opt. Lett.* **31** 999
[15] Emile O and Emile J 2014 *Appl. Phys. B* **117** 487
[16] Zhou H L, Yan S Q, Dong J J and Zhang X L 2014 *Opt. Lett.* **39** 3173
[17] Han Y J, Liao G Q, Chen L M, Li Y T, Wang W M and Zhang J 2015 *Chin. Phys. B* **24** 115203
[18] Zhang X M, Shen B F, Shi Y, Wang X F, Zhang L G, Wang W P, Xu J C, Yi L Q and Xu Z Z 2015 *Phys. Rev. Lett.* **114** 173901
[19] Denoeud A, Chopineau L, Leblanc A and Quéré F 2017 *Phys. Rev. Lett.* **118** 033902
[20] Arber T D, Bennett K, Brady C S, Douglas A L, Ramsay M G, Sircombe N J, Gillies P, Evans R G, Schmitz H, Bell A R and Ridgers C P 2015 *Plasma Phys. Contr. F.* **57** 113001
[21] Bulanov S V, Naumova N M and Pegoraro F 1994 *Phys. Plasmas* **1** 745
[22] Lichters R, MeyerterVehn J and Pukhov A 1996 *Phys. Plasmas* **3** 3425
[23] Born M and Wolf E 1999 *Principles of Optics*, 7th edn. (Cambridge: Cambridge University Press) p. 287
[24] Lipson A, Lipson S G and Lipson H 2011 *Optical Physics*, 4th edn. (Cambridge: Cambridge University Press) p. 203